INSECTA MATSUMURANA

New Series 77: 1–15 October 2021

THE EARLIEST FOSSIL RECORD OF THE SUBORDER PSOCOMORPHA (INSECTA: PSOCODEA) FROM MID-CRETACEOUS BURMESE AMBER, WITH DESCRIPTION OF A NEW GENUS AND SPECIES

By Kazunori Yoshizawa and Shûhei Yamamoto

Abstract

Yoshizawa, K. and Yamamoto, S. 2021. The earliest fossil record of the suborder Psocomorpha (Insecta: Psocodea) from mid-Cretaceous Burmese amber, with description of a new genus and species. *Ins. matsum. n. s.* 77: 1–15, 5 Figs.

We describe a new psocid genus and species, †*Burmesopsocus lienhardi* Yoshizawa, based on a fossil specimen embedded in mid-Cretaceous Burmese (Kachin) amber. Phylogenetic analysis based on the morphological data strongly suggest that the species is a member of the suborder Psocomorpha and may belong to the infraorder Homilopsocidea. However, its familial placement could not be determined. Therefore, this species is treated here as *incertae sedis* within Homilopsocidea without assigning it to any known family. This is the oldest fossil record of Psocomorpha and represents the first occurrence of the suborder from Kachin amber. The present discovery of a mid-Cretaceous homilopsocid species will contribute greatly to calibrating the time tree of Psocodea.

Authors' address. Yoshizawa, K.: Systematic Entomology, School of Agriculture, Hokkaido University, Sapporo 060–8589, Japan (corresponding author: psocid@res.agr.hokudai.ac.jp). Yamamoto, S.: The Hokkaido University Museum, Sapporo 060–0810, Japan.

INTRODUCTION

The insect order Psocodea (bark lice, book lice and parasitic lice) is subdivided into three suborders: Trogiomorpha, Troctomorpha (in which parasitic lice are classified) and Psocomorpha. Among the nonparasitic extant psocodeans (formerly called "Psocoptera", containing 41 families and ca. 6,500 species), Psocomorpha is the most diversified suborder, composed of 27 families and ca. 5,300 species (Lienhard & Smithers, 2002; Lienhard, 2016, 2021). Recent studies of amber psocids, especially those from Burmese amber (mid-Cretaceous, ca. 99 MYA), recovered high paleodiversity of the suborders Trogiomorpha and Troctomorpha in the Cretaceous Period (e.g., Mockford et al., 2013; Ross, 2019, 2020, 2021). In contrast, Cretaceous fossils of Psocomorpha are very scarce, and only two species of the suborder have been recorded from the Late Cretaceous Taimyr amber of northern Siberia (ca. 86 MYA). The systematic placement of Cretaceous psocids within the extant suborder Psocomorpha is almost doubtless for one species (*Archaelachesis granulosa* Vishniakova, 1975) but is debatable for the other (*Cretapsocus capillatus* Vishniakova, 1975) (Mockford et al., 2013).

Recent molecular phylogenetic and phylogenomic studies have provided a highly congruent and robust phylogenetic framework for Psocodea (Yoshizawa & Johnson, 2014; Johnson et al., 2018; de Moya et al., 2021). In contrast, there is significant incongruence between divergence time estimates of different analyses (Misof et al., 2014; Johnson et al., 2018; Yoshizawa et al., 2018; de Moya et al., 2021). Insufficient fossil data is one of the major problems causing the instability of dating analysis (de Moya et al., 2021). Therefore, accumulations of fossil data, especially from the most diversified suborder Psocomorpha, will contribute greatly not only to fulfilling the morphological gap observed between extant taxa but also to providing additional calibration points stabilizing the dating analyses.

In the present study, we describe a new genus and species of Psocomorpha from mid-Cretaceous Burmese amber. It represents the third psocomorphan species known from the Cretaceous and the first species of the suborder recovered from Burmese amber. We also estimated its phylogenetic position by appending morphological data obtained from the fossil specimen to a data matrix constructed on the basis of extant psocid species.

MATERIAL AND METHODS

We examined a mid-Cretaceous Kachin amber (or Burmese amber in a broader sense) specimen collected in northern Myanmar (ca. 99 MYA: Shi *et al.* 2012) (Fig. 1). The amber was polished using Roxite (Iwamoto Mineral Co., Tokyo) after trimming and grinding. The front surface of the amber piece (right side of the insect) was glued on a small cover glass using Euparol for observations and for reinforcement (the amber has a crack across the insect: Fig. 1). Observations were performed using an Olympus SZX16 (Olympus Imaging Corporation, Tokyo) binocular microscope and a Zeiss Axiophot (Carl Zeiss AG, Jena) light microscope. Photographs were taken using an Olympus E-M10II (Olympus Imaging Corporation, Tokyo) digital camera attached to the Olympus SZX16 or Zeiss Axiophot microscope. Partially focused photographs were combined using Zerene Stacker (Zerene Systems LLC, WA) to obtain images with a high depth of field. Morphological terminology followed Yoshizawa (2005). The ratio between interocular

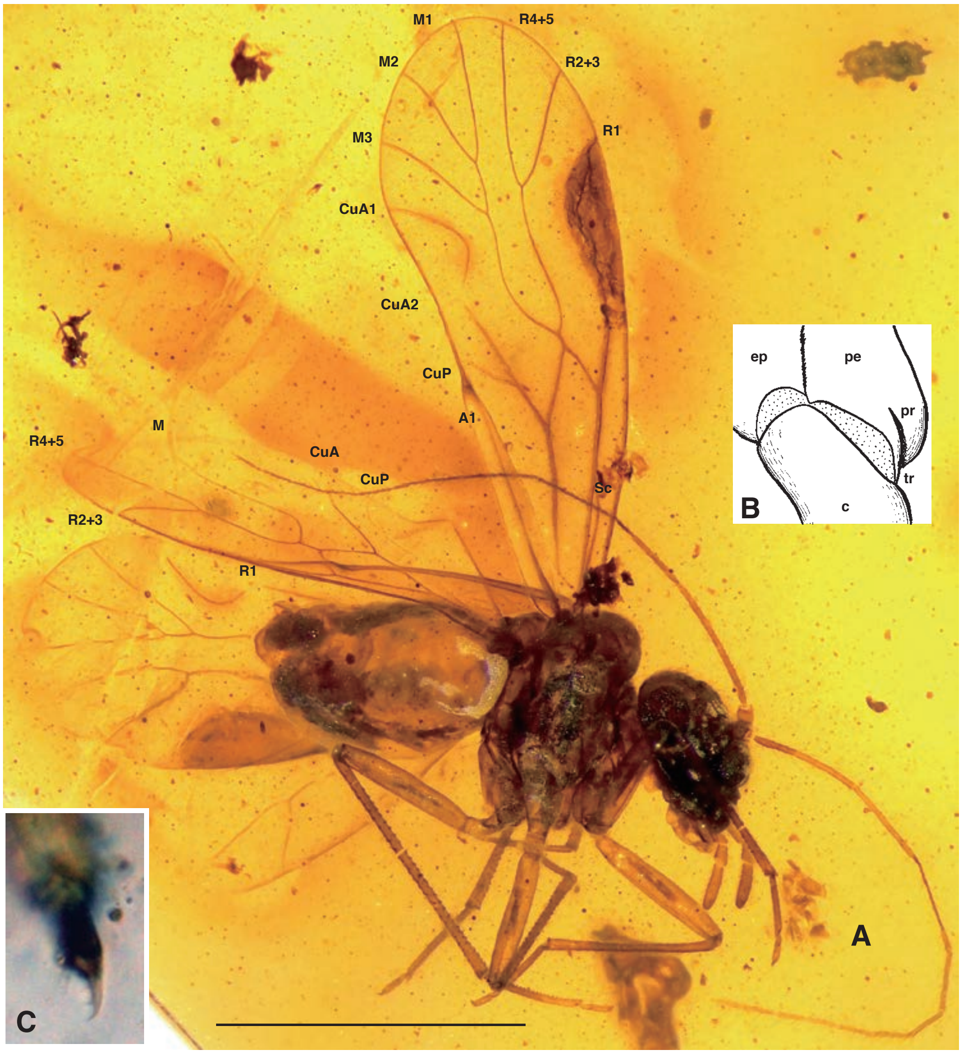

Fig. 1. *Burmesopsocus lienhardi*, n. sp. (A) Habitus (scale = 1 mm); (B) precoxal bridge (pr) and trochantin (tr) of the mesothorax. Additional abbreviations: coxa (c), epimeron (ep), preepisternum (pe); (C) pretarsal claw.

space and eye diameter (IO/D) was calculated from measurements made in frontal view of the head (Pearman, 1934)

To estimate the phylogenetic placement of this psocid species, morphological data obtained from the fossil psocid were appended to the data matrix constructed for extant species by Yoshizawa (2002) and Yoshizawa & Johnson (2014). Because significant incongruence between the trees obtained from the morphological and molecular data was identified for Psocomorpha (Yoshizawa & Johnson, 2014; de Moya et al., 2021),

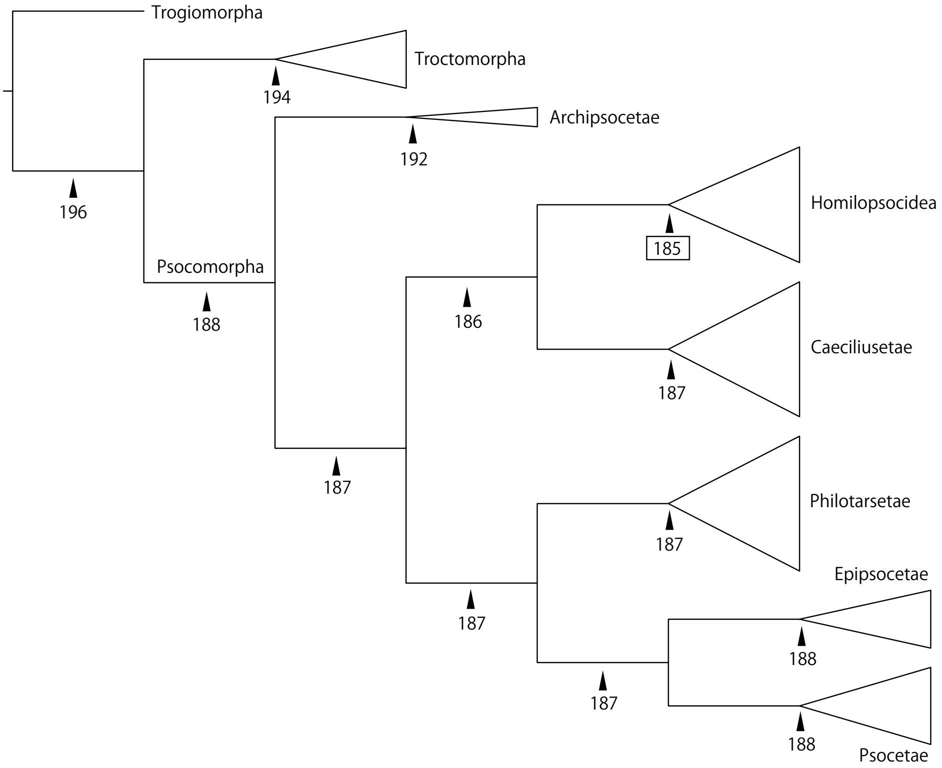

Fig. 2. Topological constraint employed in the present analyses. Arrowheads indicate all the possible positions of *Burmesopsocus* examined here, and numbers associated with the arrowheads show the tree length resulting from each constraint analysis.

we employed the constraint method for phylogenetic estimation. The monophyly of the suborders and infraorders and their relationships were constrained according to the result from a molecular phylogeny (Yoshizawa & Johnson, 2014), and the best phylogenetic position of the fossil psocid was estimated by using a heuristic search with the TBR option of PAUP* 4.0a168 (Swofford, 2004). The "backbone" constraint of PAUP* is the most efficient option for this type of analysis, but this command did not work properly. Therefore, the phylogenetic placement of the fossil psocid was examined by using the "monophyly" constraint command as follows: we performed 13 independent constraint analyses by constraining the placement of the fossil psocid to all 13 possible placements of this species (Fig. 2: within each infraorder or at all possible branches connecting the infraorders. See also constraint commands available in Appendix 2 for detail) and then compared the tree scores obtained from each analysis to decide the best placement of the fossil psocid. Character state optimization and calculation of the homoplasy indices (consistency and retention indices) were performed using MacClade 4.08 (Maddison & Maddison 2000).

TAXONOMY

Order Psocodea
Suborder Psocomorpha
Infraorder Homilopsocidea
Family *incertae sedis*
Genus *Burmesopsocus* Yoshizawa, n. gen.
(Figs 1, 3–4)

Type species. Burmesopsocus lienhardi Yoshizawa, n. sp.

Diagnosis. Within Psocomorpha, the genus *Burmesopsocus* is characterized by the combination of the following features. Head (Figs 1, 3): vertex rounded, without any concavity; postclypeus well bulged, epistomal suture complete; position of anterior tentorial pit slightly dorsal of ventral margin of cranium; mandible with rounded outer margin; galea flattened; lacinia not broadened subapically; labial palpus rounded; antenna with 11 flagellomeres. Preepisternum of prothorax not elongate; precoxal bridge of mesothorax clearly broader than base of trochantin; metapleuron with broad membranous region. Legs (Fig. 1) with fine ctenidia on hind tibia; tarsi three segmented; pretarsal claws symmetrical, with small preapical tooth, slender pulvillus and setiform basal appendix. Fore- and hindwings (Fig. 1) glabrous, with *Caecilius*-type wing shape and venation, pterostigma smoothly rounded posteriorly. Abdomen (Fig. 1) without eversible vesicles. Terminalia (Fig. 4): paraproct rounded posteriorly, trichobothrial field well developed; hypandrium simple, fused with clunium laterally; paramere well developed, aedeagus present, endopahllus with sclerotized portions but without rod-like sclerites.

Etymology. Based on superficial similarity and the phylogenetic analysis given below, this genus seems to be close to the family Mesopsocidae. The genus name refers to its origin (Burmese amber) combined with *Mesopsocus*, the type genus of Mesopsocidae.

Burmesopsocus lienhardi Yoshizawa, n. sp.
(Figs 1, 3–4)

Holotype. Male. Embedded in Kachin amber, near the Albian–Cenomanian boundary of the mid-Cretaceous, Hukawng Valley, Kachin, northern Myanmar (deposited in the Hokkaido University Insect Collection).

Description of male holotype. Body (Fig. 1) almost uniformly brown in color, except for pale membranous regions and dark portions containing internal tissue remnants.

Head (Figs 1, 3). Postclypeus well bulged, anteclypeus obvious; three ocelli arranged on flat frons; compound eye relatively small, $IO/D \approx 2.5$ (calculated from slightly inclined condition). Mouthparts: terminal segment of maxillary palpus long, approximately four times longer than width; outer tine of lacinia broad in anterior view, its ventral margin serrated, internally with distinct subapical tooth; labial palpus rounded.

Thorax as in generic diagnosis (Fig. 1).

Legs as in generic diagnosis (Fig. 1).

Wings (Fig. 1). Forewing transparent, with faint pigmentations along R, basal section of Rs, M+CuA, basal section of M, CuA, CuA1 and A1 veins, pterostigma darkly pigmented, veins dark brown except for transparent CuA2; Sc vein short, ending on R

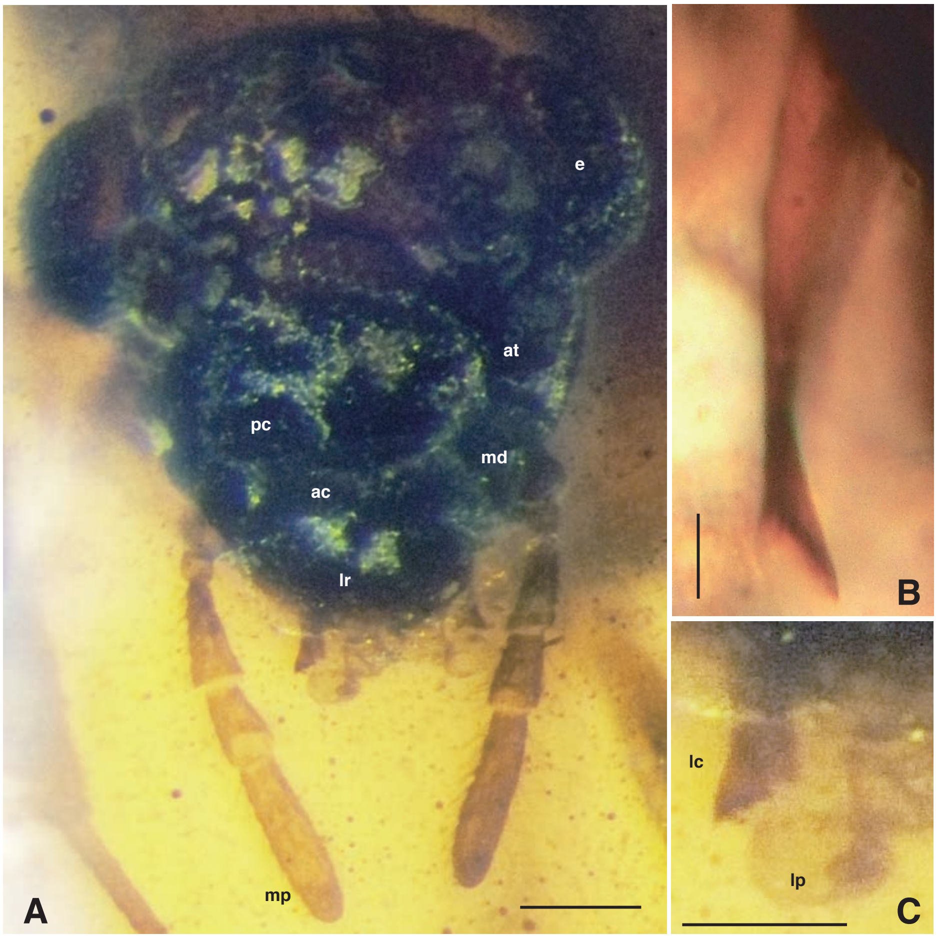

Fig. 3. Head of *Burmesopsocus lienhardi* n. sp. (A) Frontal view (scale = 0.1 mm); (B) lacinia, lateral view (scale = 0.05 mm); (C) lacinial tip and labial palpus, anterior view (scale = 0.05 mm). Abbreviations: anteclypeus (ac); anterior tentorial pit (at), compound eye (e), lacinia (lc), labial palpus (lp), labrum (lr), mandible (md), maxillary palpus (mp), postclypeus (pc).

vein; Rs and M veins fused for short distance; areola postica pointed anteriorly, highest at approximately 2/5 of its length. Hindwing transparent, veins dark brown.

Terminalia (Fig. 4). Clunium simple, without ornamentation, posterodorsal margin slightly concave, with weak swellings next to concavity. Epiproct slightly concave dorsally, with broad and smoothly curved posterior margin. Paraproct simple, posterior margin slightly concave, with distinctly convex trichobothrial field. Hypandrium with simple rounded posterior margin fused to clunium laterally. Phallosome: phallobase rounded anteriorly; parameres slightly arched; aedeagus present, but its apical condition invisible (hidden by endophallic sclerites); paired sclerotized portions of endophallus

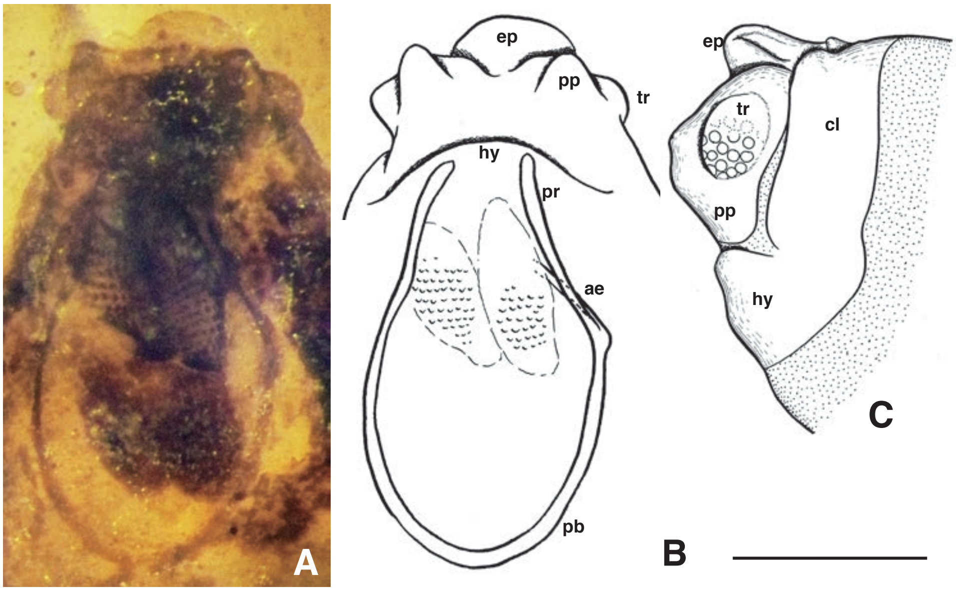

Fig. 4. Male terminalia of *Burmesopsocus lienhardi* n. sp. (scale = 0.2 mm) (A) ventral view; (B) ventral view; (C) lateral view. Abbreviations: aedeagus (ae), clunium (cl), epiproct (ep), hypandrium (hy), phallobase (pb) paraproct (pp), paramere (pr), trichobothrial field (tr).

with tiny papillate sclerotizations.

Measurements (seen from the right side of the specimen, in mm). Body 1.60; antennal flagellomeres f1 0.14, f2 0.23, f3 0.30; right forewing 1.95; right hindwing 1.52; right hind femur 0.46; right hind tibia 0.84; right hind tarsomeres t1 0.32, t2 0.05, t3 0.06.

Etymology. The specific epithet is dedicated to Charles Lienhard, a distinguished taxonomist of psocopterans and one of the most important collaborators of KY.

Phylogenetic Placement

A total of 70 characters were used for the phylogenetic estimation (Appendix 1), of which 42 characters were scored for *Burmesopsocus* but 28 were treated as missing for this taxon (most of them are female characters: Appendix 2). Among 13 possible systematic positions, the best tree score (tree length = 185) was obtained when the monophyly of *Burmesopsocus* with Homilopsocidea was constrained (Fig. 2). Under this constraint, 11 equally parsimonious trees were obtained, and their strict consensus tree corresponded to one of these 11 trees (Fig. 5).

Placement of *Burmesopsocus* within Psocomorpha and within the clade composed of all psocomorphans except for Archipsocetae were both strongly supported by several nonhomoplasious and homoplasious apomorphies (character states detected for *Burmesopsocus* indicated by asterisks in Fig. 5). The character supporting the sister-group relationship between Caeciliusetae and Homilopsocidea (Character 35:2= absence

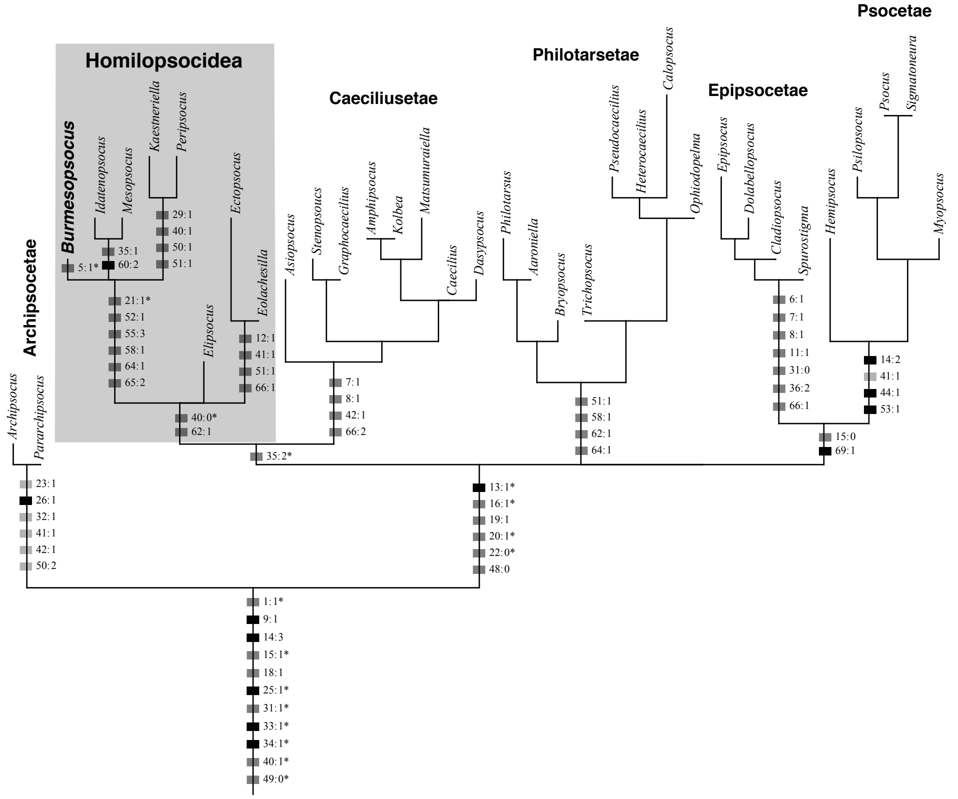

Fig. 5. The strict consensus of 11 equally parsimonious trees (identical to one of the most parsimonious trees) was estimated from the morphological data, including those from *Burmesopsocus*. The most parsimonious reconstruction of the character state changes is indicated by black (nonhomoplasious) and gray (homoplasious) bars.

of marginal setae on hindwing) was also detected for *Burmesopsocus*. Monophyly of Homilopsocidea, including *Burmesopsocus,* was supported by two apomorphies, three segmented tarsi (Character 40:0) and dorsal valve of gonapophyses with dorsal swelling (Character 62:1), but the latter is a female character so that it is not scored for *Burmesopsocus*. Within Homilopsocidea, *Burmesopsocus* formed a clade with Mesopsocidae (*Mesopsocus* and *Idatenopsocus*) and Peripsocidae (*Kaestneriella* and *Peripsocus*). This clade was supported by a total of 6 homoplasious characters; however, with the exception of one character (Character 21:1= glabrous forewing), all of them were female characters and thus were not scored for *Burmesopsocus* (Fig. 5).

DISCUSSION

The phylogenetic analyses suggested that *Burmesopsocus* is a member of the suborder Psocomorpha and belongs to the clade composed of all psocomorphans except for Archipsocetae. Both clades were supported by several apomorphies, including nonhomoplasious ones (Fig. 5). Many of them can also be observed in *Burmesopsocus*. Therefore, this placement of the genus is very strongly supported.

In contrast, the systematic placement of *Burmesopsocus* within this clade is quite ambiguous. The genus is placed in a clade composed of the infraorders Caeciliusetae and Homilopsocidea. However, only one homoplasious character (bare hindwing margin: ci=0.22, ri=0.53) was identified as an apomorphy supporting this clade. *Burmesopsocus* was further placed within the infraorder Homilopsocidea and composed a clade with Mesopsocidae (*Mesopsocus* and *Idantenopsocus*) and Peripsocidae (*Peripsocus* and *Kaestneriella*). However, all the characters supporting this clade are highly homoplasious. Furthermore, most of them are female genital characters, so they were not scored for *Burmesopsocus*. Therefore, this placement of *Burmesopsocus* is far from decisive.

However, many morphological features of *Burmesopsocus* are similar to those observed in Homilopsocidea. *Caecilius*-type venation is similar to Mesopsocidae, Elipsocidae and Lachesilidae; absence of forewing ciliation is similar to Mesopsocidae, Peripsocidae and most Lachesillidae; male genital structures, especially the shape of the phallosome, are similar to Mesopsocidae and Elipsocidae. Although most of these similarities are plesiomorphic within Psocomorpha, we concluded that Homilopsocidea is the most reasonable infraorder to place the genus *Burmesopsocus*.

In contrast, it is difficult to assign *Burmesopsocus* to any established family. Furthermore, the families Elipsocidae, Lachesillidae and Mesopsocidae (as mentioned above, *Burmesopsocus* shows morphological similarities with these taxa) are all now regarded as polyphyletic groups (Yoshizawa & Johnson, 2014; de Moya et al., 2021; Saenz Manchola et al., 2021). Therefore, the genus is treated here as *incertae sedis* without assigning it to any known family. Discovery of the female *Burmesopsocus* would be the key to deciding its systematic placement more accurately.

Two species of Cretaceous Psocomorpha, *Archaelachesis granulosa* Vishniakova, 1975 and *Cretapsocus capillatus* Vishniakova, 1975, both from the Late Cretaceous Taimyr amber (ca. 86 MYA), have been recorded to date (Mockford et al., 2013). *A. granulosa* has a strongly bulged mesothorax, which is a nonhomoplasious autapomorphy for Psocomorpha excluding Archipsocetae, so its subordinal assignment is doubtless. *C. capillatus* also has an autapomorphy of Psocomorpha (the thickened pterostigma), but this character state is also observed in a Mesozoic Troctomorpha (*Paramesopsocus* Azar et al., 2009; Mockford et al., 2013). Therefore, the assignment of *C. capillatus* to the suborder Psocomorpha is debatable. As a result, *Burmesopsocus* represents the second decisive record of the suborder Psocomorpha from the Cretaceous. *Burmesopsocus* is somewhat similar to *Archaelachesis* (known only from a female) in general morphology, including forewing venation, but differs from it by three segmented tarsi (two segmented in *Archaelachesis*: Vishniakova, 1975).

B. lienhardi is the first mid-Cretaceous psocomorphan species (vs. Late Cretaceous *Archaelachesis* and *Cretapsocus*), and its systematic placement has been firmly tested using a cladistic approach. Therefore, the fossil can be used as a new calibration point for estimating the divergence time of Psocodea. Dating analysis of Psocodea has been conducted by Johnson et al. (2018), Yoshizawa et al. (2018) and de Moya et al. (2021). The divergence date estimates of these three studies differed significantly from one another; Johnson et al. (2018) and Yoshizawa et al. (2018) estimated an age ranges of 354–328 MYA for Psocodea, 250 MYA for Psocomorpha and 194–173 MYA for

Psocomorpha ex. Archipsocetae, whereas de Moya et al. (2021) derived 192 MYA for Psocodea, 103 MYA for Psocomorpha and 70 MYA for Psocomorpha ex. Archipsocetae. In all cases, *Archaelachesis* (ca. 86 MYA) was used as the only psocomorphan calibration point for the most basal divergence. However, the present discovery clearly suggests that the divergence date of Psocomorpha ex. Archipsocetae is older than 99 MYA, showing that the divergence time derived by de Moya et al. (2021) was underestimated. The present discovery of *Burmesopsocus* and its phylogenetic placement also suggest that the ancestors of many psocomorphan infraorders originated in the mid-Cretaceous. It can be expected that further paleodiversity of Psocomorpha will be recovered in future studies, which will contribute greatly to more accurate divergence time estimation of Psocodea.

Acknowledgments

We thank Charles Lienhard for reviewing the manuscript. This study was partly supported by JSPS grants 19H03278 to KY and JP20J00159 to SY.

References

Azar, D., Hajar, L., Indary, C. & Nel, A. 2009. Paramesopsocidae, a new Mesozoic psocid family (Insecta: Psocodea: "Psocoptera: Psocomorpha). Annales de la société entomologique de France 44 (2008): 459–470 (published Jan. 31, 2009).

de Moya, R., Yoshizawa, K., Walden, K. K. O., Sweet, D. D., Dietrich, C. H. & Johnson, K. P. 2021. Phylogenomics of parasitic and non-parasitic lice (Insecta: Psocodea): Combining sequence data and exploring compositional bias in Next Generation Datasets. Systematic Biology 70: 719–738.

Johnson, K. P., Dietrich, C.H., Friedrich, F. et al. 2018. Phylogenomics and the evolution of hemipteroid insects. Proceedings of the National Academy of Science of the United States of America 115: 12775–12780.

Lienhard, C. 2016. Synthesis of parts 1–10 of the additions and corrections to Lienhard & Smithers, 2002: "Psocoptera (Insecta) – World Catalogue and Bibliography". Psocid News, Special Issue III: 1–220.

Lienhard, C. 2021. Synthesis of parts 11–21 of the additions and corrections to Lienhard & Smithers, 2002: "Psocoptera (Insecta) – World Catalogue and Bibliography". Psocid News, Special Issue IV: 1–167.

Lienhard, C. & Smithers, C. N. 2002. Psocoptera (Insecta) – World Catalogue and Bibliography. Instrumenta Biodiversitatis V, Muséum d'histoire naturelle, Genève.

Maddison, D. R. & Maddison, W. P. 2000. MacClade version 4: Computer software and user's manual. Sinauer Associates, Sunderland.

Misof, B., Liu, S., Meusemann, K. et al. 2014. Phylogenomics resolves the timing and pattern of insect evolution. Science 346: 763–767.

Mockford, E. L., Lienhard, C. & Yoshizawa, K. 2013. Revised classification of 'Psocoptera' from Cretaceous amber, a reassessment of published information. Insecta matsumurana, new series 69: 1–26.

Pearman, J. V. 1934. New and little known African Psocoptera. Stylopus 3: 121–132.

Ross, A.J. 2019. Burmese (Myanmar) amber checklist and bibliography 2018. Palaeoentomology 2 (1), 22–84.

Ross, A.J. 2020. Supplement to the Burmese (Myanmar) amber checklist and bibliography, 2019. Palaeoentomology 3 (1), 103–118.

Ross, A.J. 2021. Supplement to the Burmese (Myanmar) amber checklist and bibliography,

2020. Palaeoentomology 4 (1), 57–76.

Saenz Manchola, O. F., Herrera, S. V., D'Alessio, L. M., Yoshizawa, K., García Aldrete, A. N. & Johnson, K. P. 2021. Mitochondrial genome within barklice (Insecta: Psocodea: Psocomorpha) reveal novel gene rearrangements containing phylogenetic signal. Systematic Entomology 46: 938–951.

Shi, G., Grimaldi, D. A., Harlow, G. E., Wang, J., Wang, J., Yang, M., Lei, W., Li, Q. & Li, X. 2012. Age constraint on Burmese amber based on U–Pb dating of zircons. Cretaceous Research 37: 155–163.

Swofford, D. L. 2004. PAUP* Phylogenetic Analysis Using Parsimony (*and Other Methods). Version4. Sinauer Inc., Sunderland.

Vishniakova, V. N. 1975. Psocoptera from Late Cretaceous insect bearing resins of the Taimyr. Entomologicheskoe Obozrenie 54: 92–106.

Yoshizawa, K. 2002. Phylogeny and higher classification of suborder Psocomorpha (Insecta: Pscodea: "Psocomorpha"). Zoological Journal of the Linnean Society 136: 371–400.

Yoshizawa, K. 2005. Morphology of Psocomorpha (Psocodea: 'Psocoptera'). Insecta matsumurana, new series 60: 1–44.

Yoshizawa, K. & Johnson, K. P. 2014. Phylogeny of the suborder Psocomorpha (Insecta: Psocodea: 'Psocoptera'): congruence and incongruence between morphology and molecules. Zoological Journal of the Linnean Society 171: 716–731.

Yoshizawa, K., Johnson, K. P. Sweet, A. D., Yao, I., Ferreira, R. L. & Cameron, S. L. 2018. Mitochondrial phylogenomics and genome rearrangements in the barklice (Insecta: Psocodea). Molecular Phylogenetics and Evolution 119: 118–127.

Appendix 1. List of characters used in the present analysis and homoplasy indices obtained from it. See Yoshizawa (2002) and Yoshizawa & Johnson (2014) for details.

1: Vertex. (0) sharply angled; (1) rounded. ci=0.33; ri=0.67.
2: Vertex. (0) without concavity; (1) with pair of concavities. ci=1; ri=1.
3: Internal ridge of epistomal suture. (0) broad; (1) narrow. ci=0.25; ri=0.81.
4: Epistomal suture. (0) complete; (1) absent dorsally. ci=0.33; ri=0.
5: Position of anterior tentorial pit. (0) on ventral margin of cranium; (1) separated from ventral margin of cranium. ci=0.25; ri=0.77.
6. Labrum. (0) without paired longitudinal sclerites; (1) with paired longitudinal sclerites. ci=0.50; ri=0.75.
7: Mandible. (0) outer margin rounded and posterior margin not hollowed; (1) outer margin angled and posterior margin hollowed. ci=0.33; ri=0.83.
8: Galea. (0) flat; (1) ball shaped. ci=0.33; ri=0.83.
9: Stipito–galeal muscle (s–g7). (0) present; (1) absent. ci=1; ri=1.
10: Lacinia. (0) without a broadened region; (1) with an externally broadened subapical region. ci=1; ri=0.
11: Labial palpus. (0) rounded; (1) triangular. ci=0.50; ri=0.90.
12: Preepisternum of prothorax. (0) short; (1) elongate. ci=0.50; ri=0.88.
13: Mesothorax. (0) not strongly bulged; (1) greatly bulged dorsally. ci=1; ri=1.
14: Mesothoracic dorso–ventral flight muscle. (0) composed of one or two muscles, and inserted onto the base of trochantin; (1) divided into three muscles: external two inserted onto the precoxal bridge and internal one onto trochantin; (2) divided into three muscles: internal two inserted onto the precoxal bridge and external one onto trochantin. ci=1; ri=1.
15: Precoxal bridge. (0) narrow; (1) broad. ci=0.50; ri=0.92.
16: Membranous region of metapleuron. (0) narrow; (1) broad.ci=0.50; ri=0.92.
17: Campaniform sensilla on forewing radius. (0) evenly distributed; (1) divided into two groups. ci=0.50; ri=0.86.
18: Apex of first axillary sclerite of forewing. (0) without minute process proximally; (1) with minute process proximally; (2) broadened. ci=0.67; ri=0.89.
19: Second axillary sclerite (2Ax) and proximal median plate (PMP) of forewing. (0) articulated with each other; (1) fused with each other. ci=0.50; ri=0.86.
20: Posterior margin of folded forewings proximal to nodulus. (0) closely approximated with each other; (1) separated from each other. ci=0.50; ri=0.86.
21: Forewing margin and veins. (0) setose; (1) bare. ci=0.20; ri=0.56.
22: Membranous region of forewing. (0) bare; (1); sparsely setose; (2) densely setose. ci=0.40; ri=0.50.
23: Marginal setae of forewing. (0) not crossing; (1) crossing on apical margin. ci=0.33; ri=0.71.
24: Setae on veins of forewing. (0) 0–1 row; (1) 2 or more rows. ci=0.25; ri=0.77.
25: Pterostigma. (0) not thickened; (1) thickened. ci=1; ri=1.
26: Forewing veins. (0) normal; (1) reduced. ci=1; ri=1.
27: Forewing R_1–R_{2+3} cross vein. (0) absent; (1) present. ci=1; ri=1.
28: Forewing Rs and M. (0) fused; (1) connected by cross vein. ci=1; ri=1.
29: Areola postica. (0) present; (1) absent. ci=0.50; ri=0.50.
30: Forewing veins CuA_1 and M. (0) free from each other; (1) connected by crossvein; (2) fused with each other. ci=0.50; ri=0.50.
31: Forewing vein A_2. (0) present; (1) absent. ci=0.25; ri=0.50.
32: Ventral setae of forewing. (0) absent; (1) present. ci=0.25; ri=0.67.
33: Stigmapophysis. (0) absent; (1) present. ci=1; ri=1.

34: In-flight wing coupling system. (0) a set of pointed, separated spines or truncated spines set closely together; (1) a hook composed of truncated spines fused at their base. ci=1; ri=1.

35: Marginal setae of hindwing. (0) setose all around; (1) setose between R_{2+3} and R_{4+5} only; (2) bare. ci=0.22; ri=0.53.

36: Setae on hindwing veins. (0) bare; (1) one row; (2) two rows. ci=0.50; ri=0.80.

37: Hindwing Rs and M. (0) fused; (1) connected by cross vein. ci=1; ri=0.

38: Hindwing Rs and M+Cu. (0) fused with each other basally; (1) separated from each other basally. ci=0.33; ri=0.33.

39: Ctenidia of hind tibia. (0) fine; (1) broad. ci=1; ri=1.

40: Tarsus. (0) three-segmented; (1) two-segmented. ci=0.14; ri=0.57.

41: Pulvillus. (0) fine; (1) broad; (2) absent. ci=0.14: ri=0.67.

42: Preapical tooth on pretarsal claw. (0) present; (1) absent. ci=0.20; ri=0.71.

43: Abdominal eversible vesicles. (0) absent; (1) present. ci=0.33; ri=0.80.

44: Male paraproct. (0) rounded; (1) with distal process. ci=1; ri=1.

45: Hypandrium. (0) fused with clunium laterally; (1) articulated with clunium laterally. ci=0.33; ri=0.67.

46: Hypandrial lateral bristles. (0) absent; (1) present. ci=1; ri=1.

47: Pair of lateral hypandrial processes. (0) absent; (1) present. ci=1; ri=1.

48: Apex of aedeagus. (0) pointed; (1) rounded. ci=0.25; ri=0.57.

49: Aedeagus. (0) present; (1) absent. ci=0.25; ri=0.25.

50: Paramere. (0) rod-like; (1) strap-like; (2) reduced. ci=0.67; ri=0.80.

51: Endophallus. (0) without rod-like sclerite; (1) with rod-like sclerites. ci=0.20; ri=0.56.

52: Female epiproct. (0) rounded; (1) squared. ci=0.50; ri=0.80.

53: Female paraproct. (0) rounded; (1) with conical distal projection. ci=1; ri=1.

54: Apex of dorsal valve of gonapophyses. (0) not strongly extended posteriorly; (1) strongly extended posteriorly to reach posterior margin of paraproct. ci=1; ri=1.

55: Dorsal extension of subgenital plate. (0) absent; (1) weakly projected pair of tubercles bearing a few apical setae; (2) well developed, bilobed; (3) well developed, single lobed. ci=0.60; ri=0.80.

56: Ventral extension of subgenital plate. (0) absent; (1) present. ci=1; ri=1.

57: Spermathecal sac. (0) without lateral pouch; (1) with lateral pouch at junction of sac and duct. ci=1; ri=1.

58: Gonapophyses (0) dorsal and ventral valves do not form the ovipositor; (1) dorsal and ventral valves form the ovipositor together with the egg guide of the subgenital plate. ci=0.25; ri=0.80.

59: Ventral valve of gonapophyses. (0) present; (1) absent. ci=0.33; ri=0.50.

60: Apex of ventral valve of gonapophyses. (0) tapered; (1) with dorsal lobe; (2) swollen. ci=1; ri=1.

61: Dorsal valve of gonapophyses. (0) well developed; (1) reduced to membranous lobe; (2) absent. ci=1; ri=0.

62: Dorsal region of dorsal valve of gonapophyses. (0) not swollen; (1) swollen. ci=0.50; ri=0.93.

63: Ventral region of dorsal valve of gonapophyses. (0) without swelling; (1) with swelling. ci=1; ri=1.

64: Dorsal swelling of dorsal valve of gonapophyses. (0) membranous; (1) sclerotized. ci=0.50; ri=0.50.

65: Dorsal swelling of dorsal valve of gonapophyses. (0) lobe-like; (1) forming rounded plate; (2) forming squared plate. ci=0.67; ri=0.90.

66: External valve of gonapophyses. (0) broad; (1) narrowed; (2) reduced. ci=0.67; ri=0.95.

67: Dorsal and external valves of gonapophyses. (0) separated; (1) partly fused; (2) completely united. ci=0.67; ri=0.92.
68: Posterior lobe of external valve. (0) absent; (1) present. ci=1; ri=1.
69: Mesothoracic dorso–ventral flight muscle. (0) single muscle on trochantin; (1) two muscles on trochantin. ci=1; ri=1.
70: Mesothoracic dorso–ventral flight muscle. (0) no muscle on precoxal bridge; (1) single muscle on precoxal bridge; (2) two outer muscles on precoxal bridge; (3) two internal muscles on precoxal bridge. ci=0.72; ri=0.92.

Appendix 2. Nexus formatted data matrix used for the present analysis.

```
#NEXUS
BEGIN DATA;
      DIMENSIONS NTAX=40 NCHAR=70;
      FORMAT SYMBOLS= " 0 1 2 3" MISSING=? GAP=-;
MATRIX
[                                10        20        30        40        50        60        70]
1Burmesopsocus          10?01?00?0001?11???1100010000010112000000000000??00???????????????????
2Echmepteryx            00000000000001000000020?00000000000000000000000?1000000011000000000000
3Tapinella              0000000000000?000000000?0000000000200000000000010000000000000000000000
4Troctopsocidae_Gen.    00000000000001000000100?0000000000200000000000010000000000000000000000
5Tineomorpha            00000000000001000000020?00000000000000000000000?1000000000000000000000
6Paramphientomum        00000000000001000000020?00000010000000000000000?1000000000000000000000
7Archipsocus            10000000100003100100021?11000011110000011100000102000000001?2000000003
8Pararchipsocus         10000000100003100100021?11000011110000011100000102000000001?0000000003
9Philotarsus            1010100010001311011100111000001111010100000010010001003001000101200002
0Aaroniella             1010100010001311011100111000001111010100000000010011003001000101200002
1Trichopsocus           1010100010001311021100011000001011000101111000000010000001000101100002
2Pseudocaecilius        1010100010001311021100111000001011010001111011100000002001010101100002
3Ophiodopelma           1010100010001311021100111000001011010001110011000010002001010101100002
4Heterocaecilius        1010100010001311021100111000001011010001111011100010002001010101100002
5Calopsocus             0010101110001311021101111000001011010001101011100010002001010101100002
6Bryopsocus             ???????????????????101001000001?1?0????0?0?0000000100030?100010?200002
7Epipsocus              1011111110101301011100011001001111020001000000000000000000001?0000012011
8Dolabellopsocus        1010111110101301011100011001000011020001100000000000000000001?0000012011
9Cladiopsocus           10101111101013010111000110010000110200010000000??000000000000000012011
0Spurostigma            1010111110101301011100011000000011020001000000000000000000000000011011
1Hemipsocus             10110000100012000200000010000110110000011001000?1000100000000000000010
2Psilopsocus            1010000010001201011110001000001011200010100100010200100 1?1000010000010
3Psocus                 1010100010001201011110001000021011200011000110000200100101000010000110
4Sigmatoneura           1010100010001201011110001000021011200011000110000200100101000010000110
5Myopsocus              10100000100012010111100010000210112000101001000?1000110100000000000010
6Elipsocus              1000000010001311011100001000001011100000000000000010000000010000000002
7Ectopsocus             1010000010011311011100001000101011201001110000000010002000000100010002
8Eolachesilla           1010000010011311011100001000001011200000100000000010000000000100010002
9Idatenopsocus          1000000010001311011110001000001011100100000000000000100300102010120000 2
0Mesopsocus             1000000010001311011110001000001011100000000000001000100300102010120000 2
1Kaestneriella          1011000010001311011100001000101011200001000000000111003001000101200002
2Peripsocus             1010000010001311111110001000101011000001000000000111003001000101200002
3Asiopsocus             1?10?111?1???31????11000100000101?2000?101?0??0000000000000?100002?002
4Stenopsoucs            10000011101113111111100001010011011100001110000000000000100000000 2?002
5Graphocaecilius        10000011101113111111100001010011011200001110000000000000100000000 20002
6Amphipsocus            11000011101113111111100011000001111020001110000000000000000000000 2?002
7Kolbea                 11000011101113111111100011000001111020001110000000000000000000000 2?002
8Matsumuraiella         11000011101113111111101011000001111100001110000000000000000000000 20002
9Caecilius              10000011101113111111100001000001111000001110000000000000000000000 2?002
0Dasypsocus             00000011101113111111100001000001111000001110000000000000000000000 2?002
;
END;
```

```
Begin sets;
const Homi [monophyly] = (2,((3-6),((7,8),(((9-16),((17-20),(21-25))),((1,26-32),(33-40)))))) [185]
const Cae  [monophyly] = (2,((3-6),((7,8),(((9-16),((17-20),(21-25))),((26-32),(1,33-40)))))) [187]
const HoCa [monophyly] = (2,((3-6),((7,8),(((9-16),((17-20),(21-25))),(1,(26-32),(33-40)))))) [186]
const Pso  [monophyly] = (2,((3-6),((7,8),(((9-16),((17-20),(1,21-25))),((26-32),(33-40)))))) [188]
const Epi  [monophyly] = (2,((3-6),((7,8),(((9-16),((1,17-20),(21-25))),((26-32),(33-40)))))) [188]
const PsEp [monophyly] = (2,((3-6),((7,8),(((9-16),(1,(17-20),(21-25))),((26-32),(33-40)))))) [187]
const Phil [monophyly] = (2,((3-6),((7,8),(((1,9-16),((17-20),(21-25))),((26-32),(33-40)))))) [187]
const PPE  [monophyly] = (2,((3-6),((7,8),((1,(9-16),((17-20),(21-25))),((26-32),(33-40)))))) [187]
const PexA [monophyly] = (2,((3-6),((7,8),(1,((9-16),((17-20),(21-25))),((26-32),(33-40)))))) [187]
const Arch [monophyly] = (2,((3-6),((1,7,8),(((9-16),((17-20),(21-25))),((26-32),(33-40)))))) [192]
const Psom [monophyly] = (2,((3-6),(1,(7,8),(((9-16),((17-20),(21-25))),((26-32),(33-40)))))) [188]
const Troc [monophyly] = (2,((1,3-6),((7,8),(((9-16),((17-20),(21-25))),((26-32),(33-40)))))) [194]
const Out  [monophyly] = (1,2,((3-6),((7,8),(((9-16),((17-20),(21-25))),((26-32),(33-40)))))) [196]
;
End;

BEGIN ASSUMPTIONS;
     OPTIONS DEFTYPE=unord PolyTcount=MAXSTEPS;
END;
```